ELSEVIER

Soil Dynamics and Earthquake Engineering 22 (2002) 923–930

SOIL DYNAMICS AND EARTHQUAKE ENGINEERING

www.elsevier.com/locate/soildyn

Simultaneous measurement and inversion of surface wave dispersion and attenuation curves

Carlo G. Lai[a,*], Glenn J. Rix[b,1], Sebastiano Foti[c,2], Vitantonio Roma[d,3]

[a]*Studio Geotecnico Italiano, Via Ripamonti 89, Milano, Italy*
[b]*School of Civil and Environmental Engineering, Georgia Institute of Technology, Atlanta, GA, USA*
[c]*Centre for Offshore Foundation Systems, University of Western Australia, Crawley, WA 6009, Australia*
[d]*Geodata, Spa, C.so Duca degli Abruzzi 48/E, Torino, Italy*

Abstract

Surface wave tests are non-invasive seismic techniques that have traditionally been used to determine the shear wave velocity (i.e. shear modulus) profile of soil deposits and pavement systems. Recently, Rix et al. [J. Geotech. Geoenviron. Engng 126 (2000) 472] developed a procedure to obtain near-surface values of material damping ratio from measurements of the spatial attenuation of Rayleigh waves. To date, however, the shear wave velocity and shear damping ratio profiles have been determined separately. This practice neglects the coupling between surface wave phase velocity and attenuation that arises from material dispersion in dissipative media. This paper presents a procedure to measure and invert surface wave dispersion and attenuation data simultaneously and, thus, account for the close coupling between the two quantities. The methodology also introduces consistency between phase velocity and attenuation measurements by using the same experimental configuration for both. The new approach has been applied at a site in Memphis, TN and the results obtained are compared with independent measurements.

Keywords: Surface waves; Rayleigh waves; Dispersion; Attenuation; Spectral analysis of surface waves; Shear wave velocity; Shear damping ratio; Simultaneous measurement; Simultaneous inversion

1. Introduction

Among the different types of mechanical waves that propagate in the interior and along the boundary of a soil deposit, surface waves are well suited for the development of non-invasive seismic techniques for near-surface site characterization. Surface waves originate from the condition of zero stress existing at a boundary of a half-space, which in this case is the surface of the earth. Lord Rayleigh [1] proved their existence in 1885 and highlighted the fundamental role of these waves, subsequently named Rayleigh waves, in the transmission of earthquake energy at large distances.

Some of the properties of Rayleigh waves make them particularly effective for seismic site characterization. Along the free surface of a homogeneous half-space, Rayleigh waves generated by a point source attenuate geometrically with a factor proportional to the inverse of the square root of the distance from the source. In contrast, the geometric attenuation factor of the bulk waves is proportional to the inverse of the square of the distance. Thus, at distances on the order of one to two wavelengths from the source, the contribution of bulk waves becomes negligible and the wave field is dominated by Rayleigh waves.

The displacement field of Rayleigh waves decays exponentially with depth, and it is possible to show that most of the strain energy associated with their motion is confined to a portion of the half-space within about one wavelength of the free surface[4] [2]. Hence, Rayleigh waves of different wavelengths penetrate to varying depths, giving rise in heterogeneous media to the phenomenon of *geometric dispersion*, by which the propagation velocity of surface waves is frequency-dependent. Geometric dispersion is the basis of the methods developed in geotechnical engineering that utilize surface waves for near-surface site characterization.

* Corresponding author. Tel.: +39-02-522-0141; fax: +39-02-569-1845.
E-mail addresses: sgi_lai@studio-geotecnico.it (C.G. Lai), glenn.rix@ce.gatech.edu (G.J. Rix), foti@cyllene.uwa.edu.au (S. Foti), vro@geodata.it (V. Roma).
[1] Tel.: +1-404-894-2292; fax: +1-404-894-2281.
[2] Tel.: +61-8-9380-7289; fax: +61-8-9380-1044.
[3] Tel.: +39-11-5810626; fax: +39-11-5810621.

[4] One means of expressing this phenomenon is the skin depth, the depth at which the amplitude decreases by a factor of $1/e$. For Rayleigh waves in a homogeneous medium, the skin depth is approximately 0.94λ.

0267-7261/02/$ - see front matter © 2002 Elsevier Science Ltd. All rights reserved.
PII: S0267-7261(02)00116-1

The first applications of surface waves for near-surface site characterization date back to the 1950s and 1960s when researchers used relatively simple experimental and interpretive methods [3–5]. During the 1980s, Professor Stokoe and co-workers at the University of Texas at Austin developed the spectral analysis of surface waves (SASW) method that utilizes modern signal processing techniques and theoretically based inversion algorithms to significantly expand the range of applications in which surface wave testing can be successfully used [6]. During the past 10 years, numerous improvements to the SASW method have been developed including the recognition of the importance of higher surface wave modes for some types of profiles [7,8]; the use of arrays of multiple receivers to enable more robust determination of dispersion curves [9–13]; and a variety of inversion algorithms [14–16].

Although engineering surface wave tests were originally developed for determining the velocity (i.e. stiffness) profile of soil deposits and pavement systems, it has recently been shown that surface wave tests can also be used to determine the material damping ratio profile of soil deposits [17–19], thereby providing for the complete characterization of small-strain dynamic properties at a site. However, to date, the stiffness and damping ratio profiles have been determined separately using different experimental and interpretive methods. More specifically, the experimental phase velocity dispersion curve, which is measured to obtain the shear wave velocity profile, is often determined using the *two-station method* based on measurements of the phase lag of Rayleigh waves propagating between two receivers. In contrast, the experimental attenuation curve, which is measured to obtain the shear damping ratio profile, is obtained using the *multi-station method* by observing the spatial attenuation of Rayleigh wave amplitudes over a linear array of receivers. Moreover, the shear wave velocity and shear damping ratio profiles are determined from separate inversions of the experimental dispersion and attenuation curves, respectively. These differences in experimental and interpretive methods neglect the close relationship between phase velocity and attenuation of seismic waves propagating in linear viscoelastic media [20].

In this paper a new approach to surface wave testing is presented in which the experimental dispersion and attenuation curves are determined simultaneously from a single set of measured displacement transfer functions using the same source–receiver array [21]. Once these curves have been determined, they are simultaneously inverted to obtain the shear wave velocity and shear damping ratio profiles at a site using a newly developed algorithm for the solution of the strongly coupled Rayleigh eigenproblem in linear viscoelastic media [20]. The new approach inherently accounts for the coupling between phase velocity and attenuation and produces results that are more self-consistent.

Section 2 describes the basis of the technique used for the simultaneous measurement of the dispersion and attenuation curves via experimental displacement transfer functions. Section 3 summarizes the main concepts of the algorithm used for the coupled inversion of surface wave dispersion and attenuation data. Finally, Sections 4–6 illustrate the new approach to surface wave testing at a site located in Memphis, TN.

2. Coupled measurement of dispersion and attenuation curves

The experimental dispersion and attenuation curves can be simultaneously determined using a single set of measurements and the same source–receiver array by introducing the concept of a displacement transfer function. In a linear system, which in this case is a linear viscoelastic medium, the ratio between an output and an input signal in the frequency domain is called the frequency response function, or transfer function, of the system [22].

The test configuration is shown in Fig. 1 and consists of a source and a co-linear array of receivers. The input signal is a vertical harmonic force $F_z\, e^{i\omega t}$, while the output signal is the vertical displacement $U_z(r, \omega, t)$ measured at a distance r from the source. For far-field measurements,[5] the vertical displacement $U_z(r, \omega, t)$ induced in a linear viscoelastic, vertically heterogeneous medium by a harmonic source $F_z\, e^{i\omega t}$ located at the ground surface can be written as Ref. [23]

$$U_z(r, \omega, t) = F_z \mathcal{G}(r, \omega) e^{i[\omega t - \Psi(r,\omega)]} \tag{1}$$

where $\Psi(r, \omega)$ is a complex-valued phase angle, $\mathcal{G}(r, \omega)$ is the geometric spreading function, and the dependence of U_z on frequency ω is parametric. Hence, the displacement transfer function $T(r, \omega)$ between the harmonic source and the receiver is given by

$$T(r, \omega) = \frac{U_z(r, \omega, t)}{F_z\, e^{i\omega t}} = \mathcal{G}(r, \omega) e^{-i\Psi(r,\omega)} \tag{2}$$

Assuming $\Psi(r, \omega) \approx K_R^*(\omega) r$ eliminates the implicit dependence of the complex-valued phase angle on the source-to-receiver distance and Eq. (2) becomes

$$T(r, \omega) = \frac{U_z(r, \omega, t)}{F_z\, e^{i\omega t}} = \mathcal{G}(r, \omega) e^{-iK_R^*(\omega) r} \tag{3}$$

where

$$K_R^*(\omega) = \frac{\omega}{V_R^*(\omega)} = \left[\frac{\omega}{V_R(\omega)} - i\alpha_R(\omega) \right] \tag{4}$$

[5] The near field is defined as the area in the vicinity of the source where the body-wave field is of the same order of magnitude as the surface-wave field. Numerical studies have shown that depending on the variation of shear wave velocity with depth, near-field effects are important up to a distance from the source from one-half to two wavelengths.

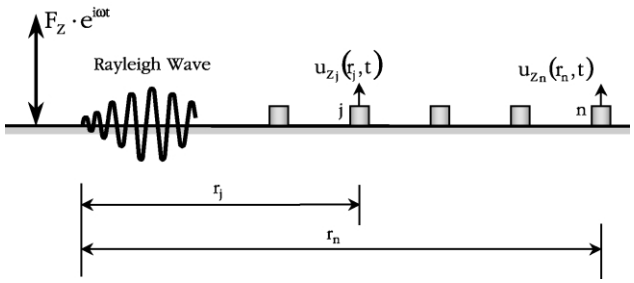

Fig. 1. Source–receivers configuration used for SASW multi-station measurements.

The assumption $\Psi(r,\omega) \approx K_R^*(\omega)r$ is equivalent to considering the phase angle $\Psi(r,\omega)$ to be the result of a single mode of propagation.

Eq. (3) can be used as a basis of a non-linear regression analysis for determining the complex-valued wavenumber $K_R^*(\omega)$. Mathematically, $K_R^*(\omega)$ is obtained by minimizing the misfit between the experimental and the predicted displacement transfer functions at a given frequency ω

$$\sum_N \left\{ \left[T(r,\omega) - \mathcal{G}(r,\omega) e^{-iK_R^*(\omega)r} \right] \mathrm{conj}\left[T(r,\omega) - \mathcal{G}(r,\omega) e^{-iK_R^*(\omega)r} \right] \right\} = \min \quad (5)$$

where N is the total number of data and conj(·) denotes the complex conjugation operator. The algorithm used for implementing Eq. (5) is the Levenberg–Marquardt method [33]. The particularly simple form of the partial derivative of Eq. (3) with respect to $K_R^*(\omega)$ makes the implementation of this algorithm very efficient. The analysis yields a series of complex-valued wavenumbers that are used to define the experimental dispersion and attenuation curves via Eq. (4).

In the implementation of the algorithm there is a difficulty associated with the fact that the geometric spreading function $\mathcal{G}(r,\omega)$ in Eq. (3) is not known a priori because it depends on the still-undetermined shear wave velocity profile. This difficulty can be overcome by means of an iterative procedure. Initially the experimental dispersion and attenuation curves are obtained from Eq. (5) with a geometric spreading function $\mathcal{G}(r,\omega)$ assumed proportional to $1/\sqrt{r}$, which is the geometric spreading relation for Rayleigh waves in homogeneous media. These curves are inverted using the procedure described subsequently to obtain approximate profiles of shear wave velocity and material damping ratio that are then used to calculate an improved estimate of $\mathcal{G}(r,\omega)$. The subsequent iteration uses the updated $\mathcal{G}(r,\omega)$ to determine new dispersion and attenuation curves from Eq. (5). This procedure is repeated until convergence. In normally dispersive media at any frequency and in inversely dispersive media at frequencies less than the cut-off frequency of the second Rayleigh mode, $\mathcal{G}(r,\omega)$ does not differ significantly from a term proportional to $1/\sqrt{r}$, and the iterative scheme converges rapidly [21].

In summary, this method determines the apparent Rayleigh phase velocities and attenuation coefficients simultaneously using displacement transfer functions $T(r,\omega)$ measured over the same linear array of receivers. Thus, it provides consistency between phase velocity and attenuation measurements. Additional details of the method and comparisons with dispersion and attenuation curves measured using conventional methods are presented in Ref. [21].

3. Coupled inversion of dispersion and attenuation curves

The shear wave velocity and shear damping ratio profiles at a site have been traditionally determined from separate (i.e. uncoupled) inversions of the dispersion and attenuation curves, respectively. Rix and Lai [18] developed a technique for determining the shear wave velocity and shear damping ratio profiles at a site from the simultaneous inversion of the experimental dispersion and attenuation curves. Their method is based on the application of a newly developed algorithm for the solution of the strongly coupled Rayleigh eigenproblem in linear viscoelastic media [20].

The coupled inversion of surface wave data offers two major advantages over the corresponding uncoupled analysis. First, it explicitly recognizes the inherent coupling existing in dissipative media between the velocity of propagation of seismic waves and material damping as a consequence of material dispersion. Secondly, the simultaneous inversion is a better-posed mathematical problem (in the sense of Hadamard) [23]. In the coupled formulation, the medium is assumed to behave as a linear viscoelastic continuum characterized by the following complex-valued seismic velocities [20]

$$V_\chi^*(\omega) = \frac{V_\chi(\omega)}{\sqrt{1+4D_\chi^2(\omega)}} \left[\frac{1+\sqrt{1+4D_\chi^2(\omega)}}{2} + iD_\chi(\omega) \right] \quad (6)$$

where $\chi = P, S, R$ denotes compression, shear and Rayleigh waves, respectively, and $V_\chi(\omega)$ and $D_\chi(\omega)$ are the corresponding phase velocities and material damping ratios. The latter are related to the attenuation coefficient $\alpha_\chi(\omega)$ by means of the expression

$$D_\chi(\omega) = \left[\frac{\frac{\alpha_\chi(\omega)V_\chi(\omega)}{\omega}}{1-\left(\frac{\alpha_\chi(\omega)V_\chi(\omega)}{\omega}\right)^2} \right] \quad (7)$$

The coupled inversion of the experimental dispersion and attenuation curves is performed by applying the complex formalism to a constrained least squares algorithm that enforces maximum smoothness of the resulting complex-valued shear wave velocity profile of the site [18]. This type of local-search algorithm has been shown to be more robust for the solution of non-linear inverse problems than traditional least squares algorithms [24].

The solution is found by expanding the non-linear relationship $\mathbf{V}_R^*(\omega) = \mathbf{V}_R^*(\mathbf{V}_S^*)$ between the complex-valued

vector $\mathbf{V}_{\mathrm{R}}^{*}=[(V_{\mathrm{R}}^{*})_1,(V_{\mathrm{R}}^{*})_2,\ldots,(V_{\mathrm{R}}^{*})_{n_{\mathrm{F}}}]$ of experimental Rayleigh phase velocities computed using Eqs. (3)–(5) (n_{F} is the number of frequencies at which $\mathbf{V}_{\mathrm{R}}^{*}$ is measured), and the complex-valued vector $\mathbf{V}_{\mathrm{S}}^{*}=[(V_{\mathrm{S}}^{*})_1,(V_{\mathrm{S}}^{*})_2,\ldots,(V_{\mathrm{S}}^{*})_{n_{\mathrm{L}}}]$ of unknown shear wave velocities (n_{L} is the number of layers of the soil deposit) in a Taylor series about an initial complex-valued shear wave velocity profile $\mathbf{V}_{\mathrm{S0}}^{*}$ and retaining terms only up to first order

$$(\mathbf{J}_{\mathrm{S}}^{*})_{\mathbf{V}_{\mathrm{S0}}^{*}}\cdot\mathbf{V}_{\mathrm{S}}^{*}=(\mathbf{J}_{\mathrm{S}}^{*})_{\mathbf{V}_{\mathrm{S0}}^{*}}\cdot\mathbf{V}_{\mathrm{S0}}^{*}+(\mathbf{V}_{\mathrm{R}}^{*}-\mathbf{V}_{\mathrm{R0}}^{*}) \tag{8}$$

where $\mathbf{V}_{\mathrm{R0}}^{*}$ is the $n_{\mathrm{F}}\times 1$ vector formed by the complex-valued Rayleigh phase velocities that are obtained by solving the equation $\mathbf{V}_{\mathrm{R}}^{*}(\omega)=\mathbf{V}_{\mathrm{R}}^{*}(\mathbf{V}_{\mathrm{S0}}^{*})$. The term $(\mathbf{J}_{\mathrm{S}}^{*})_{\mathbf{V}_{\mathrm{S0}}^{*}}$ is the $n_{\mathrm{F}}\times n_{\mathrm{L}}$ Jacobian matrix whose elements are the complex-valued partial derivatives $[\partial(V_{\mathrm{R}}^{*})_j/\partial(V_{\mathrm{S}}^{*})_k]_{\mathbf{V}_{\mathrm{S0}}}$ ($j=1,n_{\mathrm{F}}$; $k=1,n_{\mathrm{L}}$). These partial derivatives are obtained using closed-form expressions derived from the variational principle of Rayleigh waves extended to a viscoelastic medium [25].

Eq. (8) may be solved iteratively to refine the initial complex-valued shear wave velocity profile $\mathbf{V}_{\mathrm{S0}}^{*}$ until convergence. The solution is sought with the constraint that the resulting $\mathbf{V}_{\mathrm{S}}^{*}$ profile should satisfy the criterion of maximum smoothness while predicting the experimental vector $\mathbf{V}_{\mathrm{R}}^{*}$ with a specified accuracy. Using the method of Lagrange multipliers, the result is [23,24]

$$\begin{aligned}\mathbf{V}_{\mathrm{S}}^{*}=\{&\mu(\boldsymbol{\partial}^{\mathrm{T}}\boldsymbol{\partial})+[\mathbf{W}^{*}\cdot(\mathbf{J}_{\mathrm{S}}^{*})_{\mathbf{V}_{\mathrm{S0}}^{*}}]^{H}\cdot[\mathbf{W}^{*}\cdot(\mathbf{J}_{\mathrm{S}}^{*})_{\mathbf{V}_{\mathrm{S0}}^{*}}]\}^{-1}\\&\cdot[\mathbf{W}^{*}\cdot(\mathbf{J}_{\mathrm{S}}^{*})_{\mathbf{V}_{\mathrm{S0}}^{*}}]^{H}\cdot\mathbf{W}^{*}\bar{\mathbf{d}}_{0}^{*}\end{aligned} \tag{9}$$

where μ may be interpreted as a smoothing parameter, $\mathbf{W}^{*}$ is a complex-valued, diagonal $n_{\mathrm{F}}\times n_{\mathrm{F}}$ matrix formed by the reciprocal of the standard deviations associated with the experimental data $\mathbf{V}_{\mathrm{R}}^{*}$, $\boldsymbol{\partial}$ is a $n_{\mathrm{L}}\times n_{\mathrm{L}}$ matrix defining the two-point finite difference operator, and $\bar{\mathbf{d}}_{0}^{*}=(\mathbf{J}_{\mathrm{S}}^{*})_{\mathbf{V}_{\mathrm{S0}}^{*}}\cdot\mathbf{V}_{\mathrm{S0}}^{*}+(\mathbf{V}_{\mathrm{R}}^{*}-\mathbf{V}_{\mathrm{R0}}^{*})$. Finally, the notation $[\cdot]^{H}$ and $[\cdot]^{T}$ denotes the Hermitian and transpose operators, respectively. The smoothing parameter μ in Eq. (9) is determined by the observation that the misfit between measured and predicted (complex-valued) Rayleigh phase velocities should equal a specified value consistent with the uncertainties present in the measured velocities. A standard measure of the misfit $\boldsymbol{\epsilon}^{2}$ is given by the weighted least-squares criterion applied to complex-valued data [26]

$$\boldsymbol{\epsilon}^{2}=[\mathbf{W}^{*}\mathbf{V}_{\mathrm{R}}^{*}-\mathbf{W}^{*}\mathbf{V}_{\mathrm{R}}^{*}(\mathbf{V}_{\mathrm{S}}^{*})]^{H}\cdot[\mathbf{W}^{*}\mathbf{V}_{\mathrm{R}}^{*}-\mathbf{W}^{*}\mathbf{V}_{\mathrm{R}}^{*}(\mathbf{V}_{\mathrm{S}}^{*})] \tag{10}$$

Once the unknown complex-valued vector $\mathbf{V}_{\mathrm{S}}^{*}$ is found, the shear wave velocities $(V_{\mathrm{S}})_k$ and shear damping ratios $(D_{\mathrm{S}})_k$ of the n_{L}-layer soil deposit are computed through the following relations

$$\begin{aligned}(V_{\mathrm{S}})_k&=\frac{[\Re(V_{\mathrm{S}}^{*})_k]^2+[\Im(V_{\mathrm{S}}^{*})_k]^2}{\Re(V_{\mathrm{S}}^{*})_k}\\(D_{\mathrm{S}})_k&=\frac{[\Re(V_{\mathrm{S}}^{*})_k]\cdot[\Im(V_{\mathrm{S}}^{*})_k]}{[\Re(V_{\mathrm{S}}^{*})_k]^2-[\Im(V_{\mathrm{S}}^{*})_k]^2}\end{aligned} \tag{11}$$

where $k=1,n_{\mathrm{L}}$ and the symbols $\Re(\cdot)$ and $\Im(\cdot)$ denote the real and imaginary parts of the argument, respectively.

In linear viscoelastic media the velocity of propagation of bulk waves V_{P} and V_{S} is frequency-dependent due to the phenomenon of material dispersion. A thorough discussion on the nature of this frequency-dependence is beyond the scope of this article. It is important to note, however, that no specific assumption was made about the frequency-dependence of V_{S}^{*} in the derivations thus far. If one desires to account for material dispersion (i.e. causal inversion), the algorithm described in this section for the solution of the Rayleigh inverse problem remains valid provided that the inversion procedure is carried out at a specified reference frequency ω_{ref}. For more details on causal inversion see Refs. [23,27,28].

Finally, note that since the solution of the Rayleigh forward problem $\mathbf{V}_{\mathrm{R}}^{*}(\omega)=\mathbf{V}_{\mathrm{R}}^{*}(\mathbf{V}_{\mathrm{S}}^{*})$ is performed with reference to a specific mode of propagation, the Jacobian matrix $(\mathbf{J}_{\mathrm{S}}^{*})_{\mathbf{V}_{\mathrm{S0}}^{*}}$ and the vector $\mathbf{V}_{\mathrm{R}}^{*}$ appearing in Eqs. (8)–(10) also refer to a specific mode. The example presented subsequently was performed using the fundamental mode since the shear wave velocity profile is normally dispersive. See Refs. [12,23,29,30] for a comprehensive discussion on the effects caused by the contributions of higher modes of propagation and the use of inversion algorithms based on apparent or effective (i.e. non-modal) phase velocities.

4. Testing site

The testing site is located on Mud Island near downtown Memphis, TN. Mud Island was originally formed by dredge spoil taken from the Mississippi River. The area currently forms a peninsula located on the northwestern edge of downtown Memphis [31]. In March 2000, six seismic cone penetration tests (SCPT) were performed on the island, including two at Site A and one at each of the remaining sites (B–E). The approximate location of the testing sites is shown in Fig. 2. Fig. 3 shows the corrected cone tip resistance, sleeve friction, penetration pore water pressure, and shear wave velocity profiles from the seismic piezocone sounding conducted at Site B. The ground water table is 8 m below the ground level. For a complete description of the results obtained from the SCPT soundings and the geotechnical characterization at Mud Island see Ref. [31].

5. Testing procedure

Surface wave tests were also performed at Mud Island Site B in July 2000. Surface waves were generated by a vertically oscillating, electro-dynamical shaker operating in swept-sine mode. The frequency range used in the field test was from 3.75 to 100 Hz. Rayleigh wave particle motion was recorded by vertical accelerometers having a frequency response from 0.10 to 300 Hz. The accelerometers were

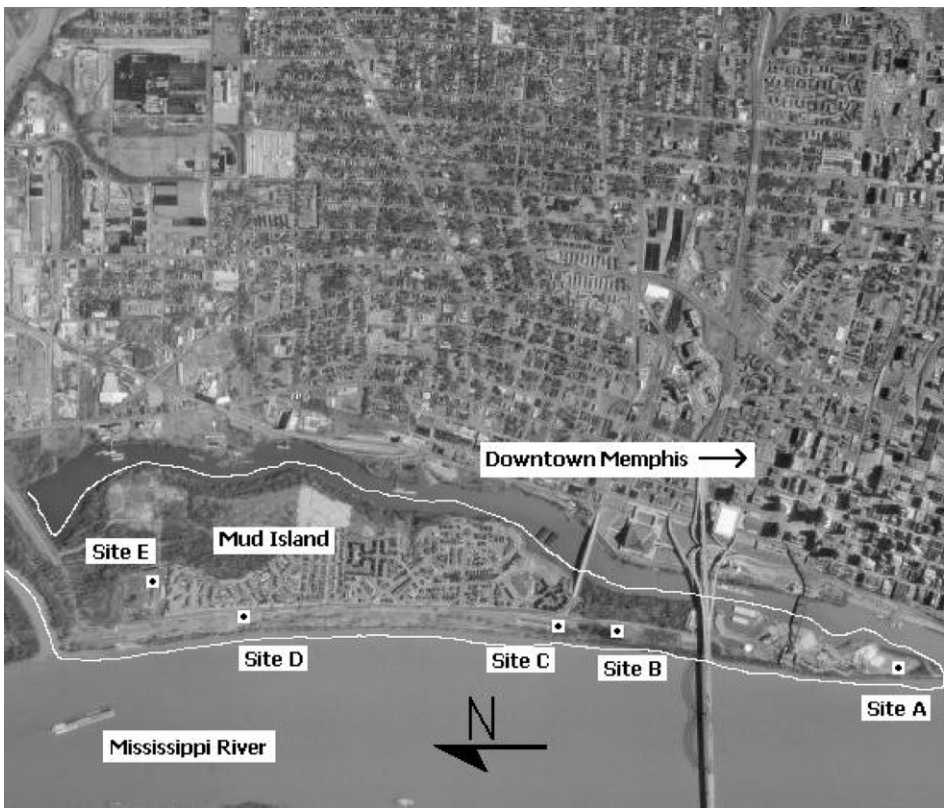

Fig. 2. Overview of the testing site locations at Mud Island, Memphis, TN (from Ref. [31]).

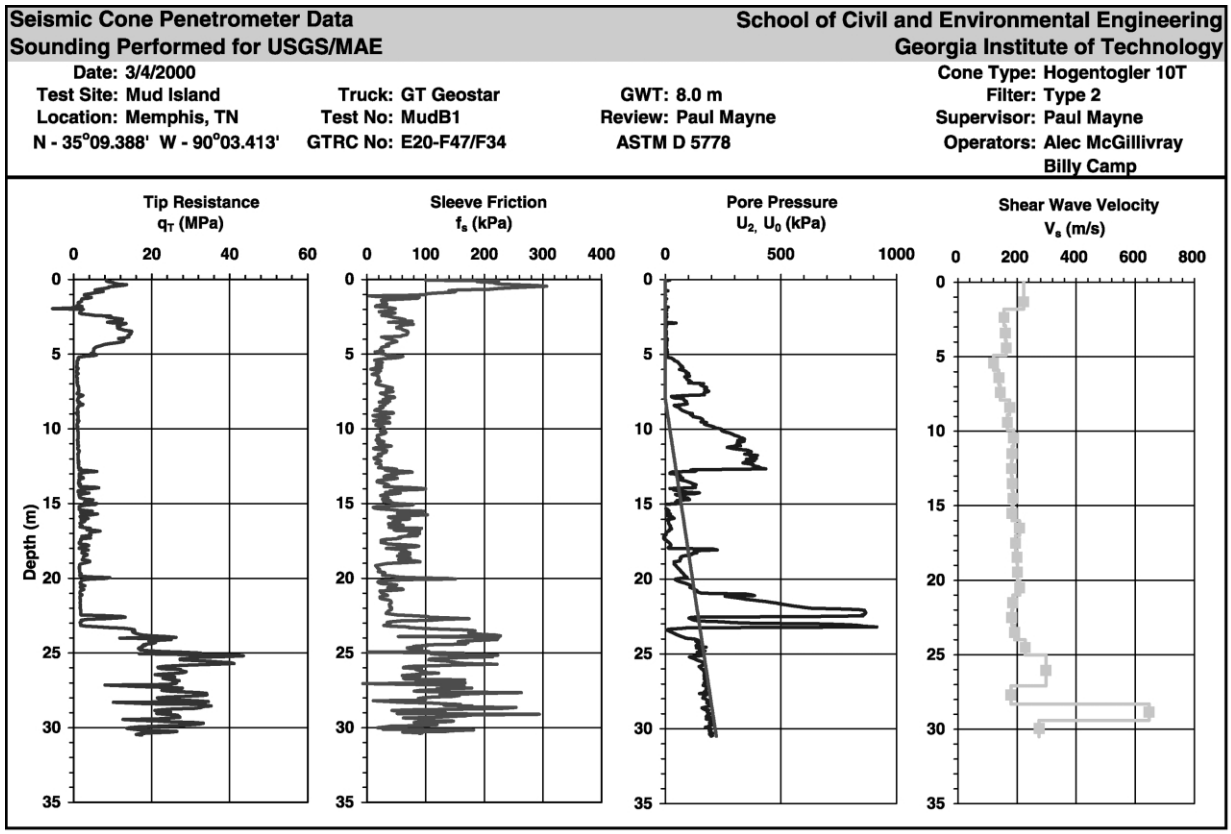

Fig. 3. Results from SCPT sounding performed at Mud Island, testing site B, Memphis, TN (from Ref. [31]).

placed in a linear array (i.e. the multi-station method) at the following offsets from the source: 2.44, 3.05, 3.66, 4.57, 5.49, 6.71, 8.54, 10.37, 12.80, 15.24, 18.29, 21.34, 24.39, 28.96, and 33.54 m. At each receiver location the experimental transfer function was obtained from an average in the frequency domain of 10 measurements to reduce the variance of the measured spectral quantities. The acceleration of the armature of the electro-dynamical shaker was also measured with a piezoelectric accelerometer to allow the input force F_z to be calculated.

The spectral quantity recorded by the dynamic signal analyzer for each receiver location was the ratio $M(r, \omega)$ of the particle acceleration measured at the receiver to the acceleration of the armature of the shaker. From $M(r, \omega)$, the experimental displacement transfer function can be readily computed by

$$T(r, \omega) = \frac{-M(r, \omega)C_2(\omega)}{\omega^2 C_1(\omega)} \tag{12}$$

where $C_1(\omega)$ and $C_2(\omega)$ are the frequency-dependent calibration factors of the accelerometers used to measure the particle motion at the receiver positions and the accelerometer placed on the shaker, respectively. The factor $C_2(\omega)$ also includes the mass of the armature to convert acceleration to force. The dynamic signal analyzer calculates the transfer function in such a way that uncorrelated output noise is eliminated [32].

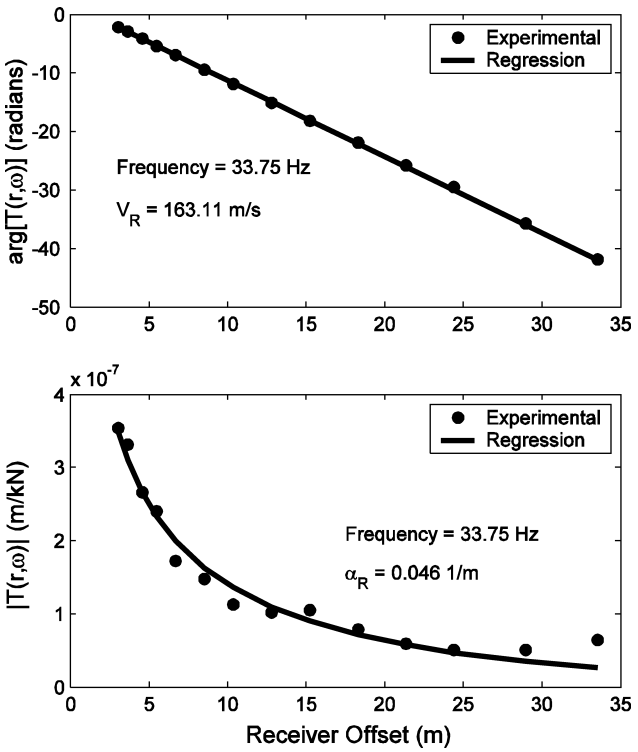

Fig. 4. Coupled transfer function regression for (a) phase velocity and (b) attenuation coefficient at 33.75 Hz at Mud Island, testing site B, Memphis, TN.

6. Results obtained at Mud Island site B

Once the experimental transfer functions were measured, the procedure described in Section 2 was used to simultaneously obtain the dispersion and attenuation curves via a non-linear regression to determine the complex-valued wavenumber at each frequency. Fig. 4 shows the results for 33.75 Hz. This analysis was repeated at other frequencies to obtain the experimental dispersion and attenuation curves shown in Fig. 5. The transfer function data were selected to minimize near-field and spatial aliasing effects, and only frequencies ranging from 5.31 to 68.75 Hz were used in the analysis.

Using the technique described in Section 3, the experimental dispersion and attenuation curves shown in Fig. 5 were simultaneously inverted to determine the shear wave velocity (V_S) and shear damping ratio (D_S) profiles shown in Fig. 6. The V_S profile compares well with the values of shear wave velocities measured at Mud Island Site B with the SCPT test. The figure shows that V_S generally increases with depth from values of approximately 180 m/s near the ground surface to about 240 m/s at 30 m depth. The values of D_S vary from about 1.5 to 3.9%. Unfortunately, no independently measured values of D_S are available for comparison, but the values obtained via surface wave testing are within the range of variation of this parameter in soils at small-strain levels [34]. At a site

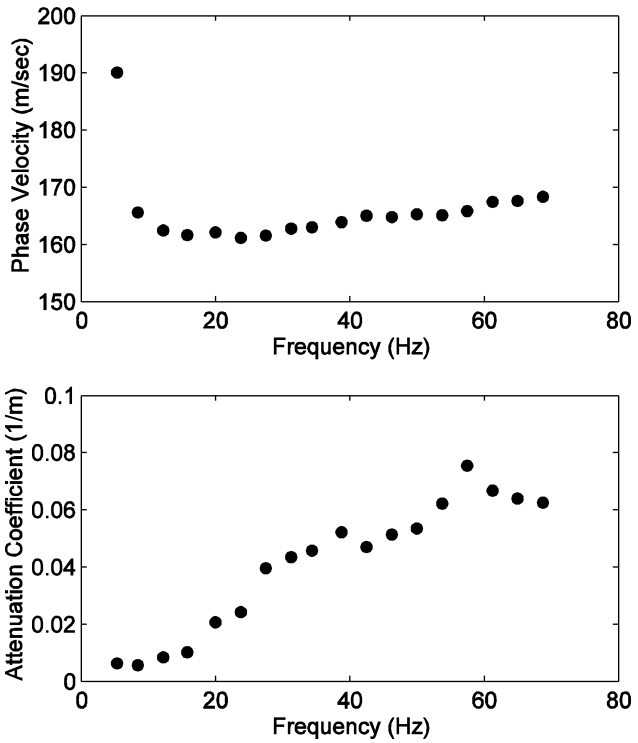

Fig. 5. Rayleigh (a) dispersion and (b) attenuation curves obtained with the coupled measurement technique at Mud Island, testing site B, Memphis, TN.

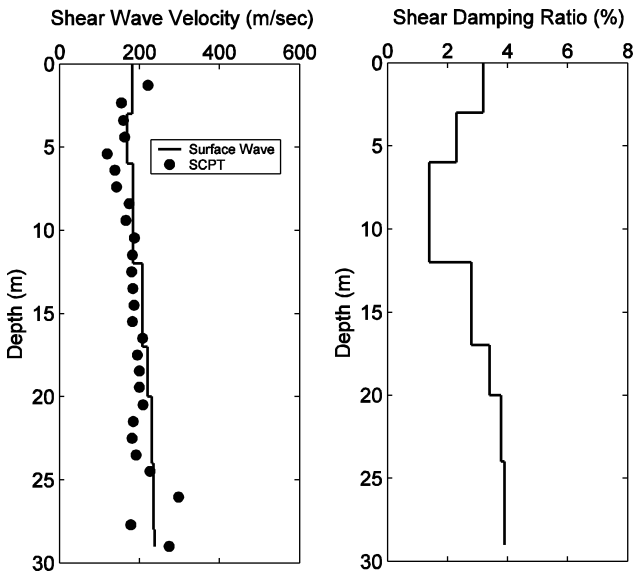

Fig. 6. Shear wave velocity and shear damping ratio profiles obtained using the simultaneous inversion algorithm at Mud Island, testing site B, Memphis, TN.

where independent values of D_S were available, the values obtained from an uncoupled inversion of surface wave attenuation data were in excellent agreement [17], providing confidence in surface-wave-based measurements.

As a check of the inversion results, Fig. 7 shows the fit between experimental dispersion and attenuation curves and the corresponding theoretical curves yielded by the simultaneous inversion algorithm at the end of the fifth and final iteration. Both the theoretical dispersion and attenuation curves are in satisfactory agreement with the curves measured experimentally.

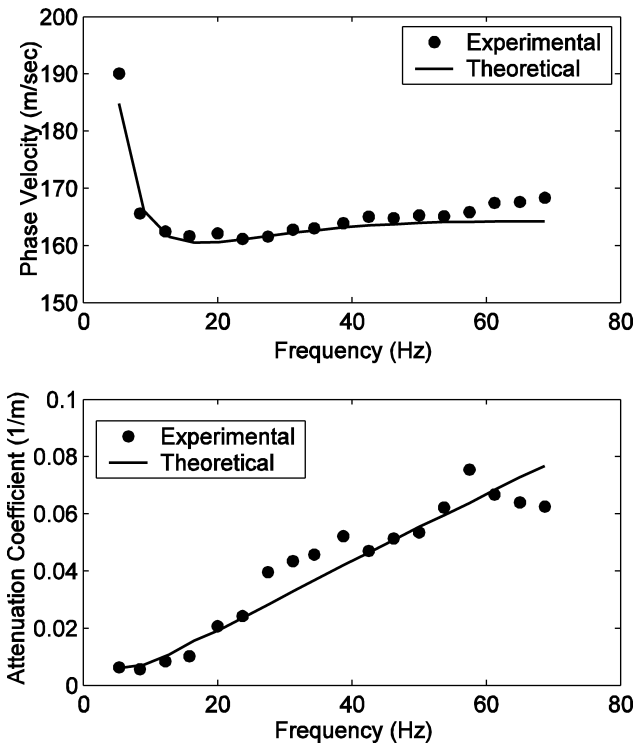

Fig. 7. Comparison between experimental and theoretical dispersion and attenuation curves (fundamental mode) at Mud Island, testing site B, Memphis, TN.

7. Conclusions

Surface wave tests are non-invasive field techniques that can be used to determine the shear wave velocity and the shear damping ratio profiles at a site. In the conventional test procedure, the experimental dispersion and attenuation curves are measured separately using different source–receiver configurations and different interpretation methods. Furthermore, the shear wave velocity and shear damping ratio profiles determined from these curves are also obtained independently using separate inversion algorithms.

In this paper an efficient and elegant procedure is proposed in which the experimental dispersion and attenuation curves are both measured and inverted concurrently from a single set of measurements using the same source–receiver array. The new approach is motivated by (1) the recognition that the phase velocity and attenuation of seismic waves are not independent as a result of material dispersion in dissipative media and (2) the desirability of providing consistency between phase velocity and attenuation measurements. The method has been applied at Mud Island B, a site near downtown Memphis, TN, where independent in situ measurements of shear wave velocity were available for comparison. The shear wave velocity profile determined with the simultaneous inversion algorithm agrees well with the independent measurements, whereas the values of shear damping ratio are in good agreement with data from the literature.

Acknowledgments

This material is based upon work supported by the National Science Foundation under Grant No. CMS-9616013. The first author would like to acknowledge Studio Geotecnico Italiano S.r.l. for the support given in performing the numerical simulations and preparing the manuscript. The authors would like to thank Dr Paul W. Mayne for providing the SCPT data used for comparison.

References

[1] Rayleigh L. On waves propagated along the plane surface of an elastic solid. Proc Lond Math Soc 1885;17:4–11.
[2] Fung YC. Foundations of solid mechanics. Englewood Cliffs, NJ: Prentice-Hall; 1965.
[3] Jones RB. In-situ measurement of the dynamic properties of soil by vibration methods. Geotechnique 1958;8(1):1–21.

[4] Ballard RF Jr. Determination of soil shear moduli at depth by in-situ vibrating techniques. Waterways Experiment Station, Miscellaneous Paper No. 4-691; 1994.
[5] Richart Jr.FE, Woods RD, Hall JR. Vibrations of soils and foundations. Englewood Cliffs, NJ: Prentice-Hall; 1970.
[6] Stokoe IIKH, Wright SG, Bay J, Roësset J. Characterization of geotechnical sites by SASW method. In: Woods RD, editor. Geophysical characterization of sites. New York/New Delhi: Oxford/IBH Publishing Co. Pvt. Ltd; 1994. p. 15–25.
[7] Gucunski N, Woods RD. Numerical simulation of the SASW test. Soil Dyn Earthquake Engng 1992;11:213–27.
[8] Tokimatsu K, Tamura S, Kojima H. Effects of multiple modes on Rayleigh wave dispersion characteristics. J Geotech Engng 1992; 118(10):1529–43.
[9] Tokimatsu K. Geotechnical site characterization using surface waves. In: Ishihara K, editor. Earthquake geotechnical engineering. Rotterdam: Balkema; 1995. p. 1333–68.
[10] Park C, Miller R, Xia J. Multichannel analysis of surface waves. Geophysics 1999;64:800–8.
[11] Zywicki DJ. Advanced signal processing methods applied to engineering analysis of seismic surface waves. PhD Dissertation, Georgia Institute of Technology; 1999.
[12] Foti S. Multi-station methods for geotechnical characterization using surface waves. PhD Dissertation, Dipartimento di Ingegneria Geotecnica e Strutturale, Politecnico di Torino, Italy; 2000.
[13] Liu H-P, Boore DM, Joyner WB, Oppenheimer RE, Warrick RE, Zhang W, Hamilton JC, Brown LT. Comparison of phase velocities from array measurements of Rayleigh waves associated with microtremor and results calculated from borehole shear-wave velocity profiles. Bull Seismol Soc Am 2000;90(3):666–78.
[14] Joh S-H. Advances in the data interpretation technique for spectral-analysis-of-surface-waves (SASW) measurements. PhD Dissertation, University of Texas at Austin; 1996.
[15] Ganji V, Gucunski N, Nazarian S. Automated inversion procedure for spectral analysis of surface waves. J Geotech Geoenviron Engng 1998;124(8):757–70.
[16] Rix GJ, Lai CG, Orozco MC, Hebeler GL, Roma V. Recent advances in surface wave methods for geotechnical site characterization. Proceedings of the XV International Conference on Soil Mechanics and Geotechnical Engineering, Lisse: A.A. Balkema; 2001. p. 499–502.
[17] Rix GJ, Lai CG, Spang AW. In situ measurements of damping ratio using surface waves. J Geotech Geoenviron Engng 2000;126(5): 472–80.
[18] Rix GJ, Lai CG. Simultaneous inversion of surface wave velocity and attenuation. In: Robertson PK, Mayne PW, editors. Geotechnical site characterization. Rotterdam: Balkema; 1998. p. 503–8.
[19] Foti S, Lai CG. Determinazione delle Proprietà dinamiche dei terreni mediante l'uso di onde superficiali. In: Parma, editor. Atti XX Convegno Nazionale di Geotecnica, Bologna: Pàtron; 1999. in Italian.
[20] Lai CG, Rix GJ. Solution of the Rayleigh eigenproblem in viscoelastic media. Bull Seismol Soc Am 2002; in press.
[21] Rix GJ, Lai CG, Foti S. Simultaneous measurement of surface wave dispersion and attenuation curves. Geotech Test J 2001;24(4):350–8.
[22] Oppenheim A, Willsky A. Signals and systems. Englewood Cliffs, NJ: Prentice-Hall; 1997.
[23] Lai CG. Simultaneous inversion of rayleigh phase velocity and attenuation for near-surface site characterization. PhD Dissertation, Department of Civil and Environmental Engineering, Georgia Institute of Technology; 1998.
[24] Constable SC, Parker RL, Constable GG. Occam's inversion: a practical algorithm for generating smooth models from electromagnetic sounding data. Geophysics 1987;52:289–300.
[25] Ben-Menahem A, Singh S. Seismic waves and sources, 2nd ed. New York: Dover; 1999.
[26] Menke W. Geophysical data analysis: discrete inverse theory. International Geophysics Series, vol. 45. New York: Academic Press; 1989. Revised Edition.
[27] Lee WB, Solomon SC. Simultaneous inversion of surface-wave phase velocity and attenuation: Rayleigh and love waves over continental and oceanic paths. Bull Seismol Soc Am 1979;69(1):65–95.
[28] Herrmann RB. Computer programs in seismology. User's manual, vol. II. Saint Louis University; 1994.
[29] Roësset JM, Chang DW, Stokoe KH II. Comparison of 2-D and 3-D models for analysis of surface wave tests. Proceedings of the Fifth International Conference on Soil Dynamics and Earthquake Engineering, Karlsruhe, Germany; 1991. p. 111–26.
[30] Roma V. Soil properties and site characterization through Rayleigh waves. PhD Dissertation, Dipartimento di Ingegneria Geotecnica e Strutturale, Politecnico di Torino, Italy; 2001.
[31] Mayne P. Results of seismic piezocone penetration tests performed in Memphis, TN. GTRC Project Nos. E-20-F47/F34 Submitted to USGS/MAE Hazard Mapping Program Central Region by Georgia Tech Research Corporation, Geosystems Engineering Group, Civil and Environmental Engineering, Atlanta, GA; 2000.
[32] Bendat J, Piersol A. Random data—analysis and measurement procedures, 2nd ed. New York: Wiley; 1986.
[33] Press WH, Teukolsky SA, Vetterling WT, Flannery BP. Numerical recipes in Fortran—the art of scientific computing, 2nd ed. Cambridge, UK: Cambridge University Press; 1992.
[34] Ishihara K. Soil behaviour in earthquake geotechnics. Oxford: Oxford Science Publications; 1996.